Time Reversal Adaptive Waveform in MIMO Radar

Yuanwei Jin
Engineering and Aviation Sciences
Univ. of Maryland, Eastern Shore
Princess Anne, MD 21853

Nicholas O'Donoughue, José M.F. Moura
Electrical and Computer Engineering
Carnegie Mellon University
Pittsburgh, PA 15213

Abstract—EM multipath propagation is common in radar and wireless communications. Most radar systems are designed assuming line-of-sight (LOS), not multipath. In this paper, we extend our prior work on Multi-Input Multi-Output (MIMO) radar in the absence of interference [1], to consider MIMO radar detection in high clutter. We develop a subspace MIMO target model and a statistical model for MIMO radar clutter that accounts for the spatial and spectral properties of radar returns. We show that, using orthogonal waveform signaling, the time reversal MIMO radar yields higher detection performance than conventional statistical MIMO radar in high clutter.

Index Terms—Time Reversal, MIMO Radar, Clutter

I. INTRODUCTION

Radar systems are typically designed for Line of Sight (LOS) conditions, where the target is directly visible to the radar platform. These systems perform reliably but are limited in the presence of multipath, which gives rise to non-LOS propagation [2]. For example, urban environments create large radar shadows, limiting LOS systems' ability to interrogate hidden targets. We develop a time-reversal approach to MIMO radar that results in a transmit waveform that is adapted to the multipath channel. The concept of waveform design or re-shaping has been studied extensively for both conventional [3] and MIMO [4] radar applications. We adopt the statistical multi-input multi-output (MIMO) radar framework from [5], [6], which utilizes spatial diversity among the transmit and receive antenna arrays to interrogate different aspect angles of the target, and incorporate statistical models for radar clutter.

In spatial MIMO architectures, diverse antenna locations result in independence of the target radar cross section (RCS) among the different transmission paths. Transmission of orthogonal waveforms from each transmitter creates an independent target measurement for each transmitter-receiver pair. Exploiting this independence allows MIMO radars to improve detection performance and radar sensitivity. This is in contrast with the conventional phased array approach, which presupposes a high degree of correlation between signals transmitted and received by an array.

We derived in [1] the concept of Time Reversal MIMO (TR-MIMO) radar, where we explored it in the simplified case of white, stationary clutter. TR-MIMO operates under heavy multipath conditions, which are often experienced in radar, sonar, and wireless communications systems. The presence of rich multipath degrades LOS conditions, and negatively impacts

conventional radar performance. In addition to MIMO radar, Time Reversal has been studied for various radar scenarios [7], [8], [9]. In this paper, we extend the results in [1] to consider the presence of clutter.

II. MIMO SYSTEM MODEL

We consider the problem of detecting a stationary or slowly moving target in the presence of rich multipath. This section is broken into two parts: target model and clutter model.

A. Target Subspace Model

The target is modeled as a point-source; we characterize RCS fluctuations by Swerling's models [10]. Through dense multipath, we assume that each transmission path experiences an independent realization of the target's RCS. We use discrete frequency samples $f_q, q = 0, \ldots, Q - 1$. The number of frequency samples Q is chosen by $Q = \frac{BW}{B_c}$, where B_c is the multipath channel's coherence bandwidth and BW is the system bandwidth. Samples separated by B_c are assumed to be independent. For simplicity, we assume that both arrays have N antennae. We let $\mathbf{H}(f_q)$ denote the forward channel response matrix between the transmit array A and the receive array B at f_q. The (i, j)-th entry of $\mathbf{H}(f_q)$ is the forward channel response from antenna A_i to B_j. Unlike the TR-MIMO target model derived in [1] that assumes that $\mathbf{H}(f_q)$ is full-rank, we assume that the target channel is known to lie in a p-dimensional subspace determined by the target scattering field, i.e.,

$$\mathbf{H}(f_q) = \left(\mathbf{A}(f_q)\mathbf{A}^H(f_q)\right)\boldsymbol{\Theta}(f_q), \qquad (1)$$

where $N \times p$ dimensional matrix $\mathbf{A}(f_q)$ is the target signal subspace. For simplicity, we assume that the p-columns of $\mathbf{A}(f_q)$ are unitary vectors and $\mathbf{A}(f_q)$ is normalized such that $\mathrm{tr}\left[\mathbf{A}^H(f_q)\mathbf{A}(f_q)\right] = p$. $\boldsymbol{\Theta}(f_q)$ is a random matrix that accounts for random variations of the wave propagation paths between each pair of transmit and receive antennae. Each entry of $[\boldsymbol{\Theta}(f_q)]_{i,j} = \theta_{ij}(f_q) \sim \mathcal{CN}\left(0, \sigma_s^2(f_q)\right)$. This model also implies that the dominant multipath signals are confined to a p-dimensional subspace. We model the backward propagation channel [1]:

$$\overline{\mathbf{H}}(f_q) = \left(\mathbf{A}(f_q)\mathbf{A}^H(f_q)\right)\overline{\boldsymbol{\Theta}}(f_q) \qquad (2)$$

$$\overline{\boldsymbol{\Theta}}(f_q) = \rho \cdot \boldsymbol{\Theta}(f_q) + \boldsymbol{\Phi}(f_q) \qquad (3)$$

where ρ is the correlation coefficient between the forward channel $\boldsymbol{\Theta}(f_q)$ and the backward channel $\overline{\boldsymbol{\Theta}}(f_q)$. The matrix $\boldsymbol{\Phi}(f_q)$ is a channel disturbance and is independent of $\boldsymbol{\Theta}(f_q)$. Its elements are independently distributed as complex

Gaussian random variables with zero mean and variance σ_ϕ^2. We impose the constraint that each entry of $\overline{\Theta}(f_q)$ has unit variance. The correlation coefficient ρ directly describes relationship between the forward and the reverse channel response that is important to time reversal. Variation of this parameter will directly affect the performance of TR-MIMO [1].

B. Clutter Model

In general, the correlation properties of a MIMO clutter model should be characterized in the spatial and spectral domains. It has been shown that a complex Gaussian model is appropriate when multipath scattering is rich [11]. If we transmit some set of waveforms $\mathbf{s}_A(f_q)$ from array A, then the received clutter response at array B is given by:

$$\mathbf{y}_c(f_q) = \mathbf{H}_c(f_q)\mathbf{s}_A(f_q), \tag{4}$$

where $\mathbf{H}_c(f_q)$ is the clutter response matrix between array A and B. Since the elements of $\mathbf{H}_c(f_q)$ are jointly complex Gaussian, the signal vector $\mathbf{y}_c(f_q)$ is also complex Gaussian:

$$\mathbf{y}_c(f_q) \sim \mathcal{CN}\left(0, \mathbf{R}_{y,c}(f_q)\right). \tag{5}$$

We define the transmit waveform:

$$\mathbf{s}_A(f_q) = [S_1(f_q), \ldots, S_N(f_q)]^T, \tag{6}$$

such that the probing signals are all orthogonal:

$$\sum_{q=0}^{Q-1} \mathbf{s}_A(f_q)\mathbf{s}_A^H(f_q) = QE_s\mathbf{I}_N, \tag{7}$$

where E_s is the probing signal energy $E_s = \frac{1}{Q}\sum_{q=0}^{Q-1}|S_i(f_q)|^2$. In [1], we model each entry of the clutter response as a complex Gaussian random variable:

$$\mathbf{H}_c(f_q) = \mathbf{\Lambda}^{1/2}\mathbf{V}(f_q), \tag{8}$$

where the matrix $[\mathbf{V}(f_q)]_{i,j} = v_{ij} \sim \mathcal{CN}\left(0, \sigma_c^2(f_q)\right)$, and

$$\mathbf{\Lambda} = \begin{bmatrix} 1 & \lambda & \cdots & \lambda^{N-1} \\ \lambda & 1 & \cdots & \lambda^{N-2} \\ \vdots & \vdots & \vdots & \vdots \\ \lambda^{N-1} & \lambda^{N-2} & \cdots & 1 \end{bmatrix} \tag{9}$$

Note that the rank of $\mathbf{\Lambda}$ is ± 1 when $\lambda = 1$, and N otherwise. The matrix $\mathbf{\Lambda}$ characterizes the spatial correlation of the clutter signal received at the array. The covariance matrix $\mathbf{R}_{y,c}(f_q)$ can be written:

$$\mathbf{R}_{y,c}(f_q) = 2E_sN\sigma_c^2(f_q)\mathbf{\Lambda}, \tag{10}$$

where $E\{\cdot\}$ is the expectation operator. We employ a Gaussian Power Spectral Density (PSD) model [12], [13]:

$$\sigma_c^2(f_q) \approx e^{-\frac{(f_q-f_c)^2}{2\Omega}}. \tag{11}$$

where Ω is the width of the Gaussian PSD, and f_c is the radar center frequency. For simplicity, we assume that the clutter samples at each frequency f_q are decorrelated due to rich multipath scattering. This assumption implies that the processing of clutter can be done independently in each individual frequency bin within the entire signal frequency band. Combining (10) with (11), the MIMO clutter is fully characterized in the spatial and spectral domains.

III. TIME REVERSAL PROCESSING

In [1], as well as [7], [8], [9], we considered the time reversal data collection in several stages. We describe these steps in this section. We begin with conventional probing, apply clutter suppression, and then perform time reversal probing.

1. Conventional Probing. We transmit $\mathbf{s}_A(f_q)$ from array A, through the channel to array B. The l-th snapshot of the received signal is:

$$\mathbf{y}_l(f_q) = \mathbf{H}(f_q)\mathbf{s}_A(f_q) + \mathbf{y}_{c,l}(f_q) + \mathbf{y}_{n,l}(f_q). \tag{12}$$

where $\mathbf{H}(f_q)\mathbf{s}_A(f_q)$ is the target response, $\mathbf{y}_{c,l}(f_q)$ is the clutter response defined in (4), and $\mathbf{y}_{n,l}(f_q)$ is an additive white Gaussian noise term distributed with:

$$\mathbf{y}_{n,l}(f_q) \sim \mathcal{CN}\left(0, \sigma_n^2\mathbf{I}_N\right). \tag{13}$$

For convenience, by (10), we define:

$$\mathbf{R}(f_q) \triangleq \frac{E_s\sigma_c(f_q)}{\sigma_n^2}\mathbf{\Lambda} + \mathbf{I}_N. \tag{14}$$

Hence,

$$\mathbf{y}_{c,l}(f_q) + \mathbf{y}_{n,l}(f_q) \sim \mathcal{CN}\left(0, \sigma_n^2\mathbf{R}(f_q)\right). \tag{15}$$

2. Clutter Suppression. The next stage is to whiten the clutter response, to allow for optimal detection. We note that $\mathbf{R}(f_q)$ is a positive definite matrix, so it can be decomposed into a product of Hermitian matrices $\mathbf{R}^{\frac{1}{2}}(f_q)\mathbf{R}^{\frac{T}{2}}(f_q)$. Thus we define the whitened signal vector

$$\tilde{\mathbf{y}}_l(f_q) = \mathbf{R}^{-\frac{1}{2}}(f_q)\mathbf{y}_l(f_q) \tag{16}$$

$$= \mathbf{R}^{-\frac{1}{2}}(f_q)\mathbf{H}(f_q)\mathbf{s}_A(f_q) + \mathbf{v}_l(f_q), \tag{17}$$

where the vector $\mathbf{v}_l(f_q)$ is our whitened clutter-plus-noise term:

$$\mathbf{v}_l(f_q) = \mathbf{R}^{-\frac{1}{2}}(f_q)\left[\mathbf{y}_{c,l}(f_q) + \mathbf{y}_{n,l}(f_q)\right] \tag{18}$$

$$\sim \mathcal{CN}\left(0, \sigma_n^2\mathbf{I}_N\right). \tag{19}$$

In conventional processing, the signal $\tilde{\mathbf{y}}_l(f_q)$ is used to detect the presence of a target. For time reversal, however, we have an additional step.

3. Time Reversal Subspace Signal Probing. For time reversal, the clutter whitened signal is time-reversed, energy normalized, and retransmitted from array B to array A. We define the TR probing signal:

$$\mathbf{s}_{tr,l}(f_q) = k_l\left[\mathbf{P}_{\mathbf{A}(f_q)}\tilde{\mathbf{y}}_l(f_q)\right]^*. \tag{20}$$

where $\mathbf{P}_{\mathbf{A}(f_q)} = \mathbf{A}(f_q)(\mathbf{A}^H(f_q)\mathbf{A}(f_q))^{-1}\mathbf{A}^H(f_q)$ is a projector onto the signal subspace $\mathbf{A}(f_q)$. The energy normalization term is defined by:

$$k_l^2 = \frac{\sum_{q=0}^{Q-1}\|\mathbf{s}_A(f_q)\|^2}{\sum_{q=0}^{Q-1}\left\|\mathbf{P}_{\mathbf{A}(f_q)}\tilde{\mathbf{y}}_l(f_q)\right\|^2} = \frac{QNE_s}{\sum_{q=0}^{Q-1}\left\|\mathbf{P}_{\mathbf{A}(f_q)}\tilde{\mathbf{y}}_l(f_q)\right\|^2}. \tag{21}$$

We note that (20) is a generalized DORT (decomposition of the time-reversal operator) implementation. In DORT, the transfer function of the medium can be estimated by decomposition of the time-reversal operator obtained by a set of initial transmissions [14], [15]. The received signal vector at array A is:

$$\mathbf{x}_l(f_q) = k_l \overline{\mathbf{H}}^T(f_q)\mathbf{s}_{tr,l}(f_q) + \mathbf{x}_{c,l}(f_q) + \mathbf{x}_{n,l}(f_q), \quad (22)$$

where $\mathbf{x}_{c,l}(f_q)$ is the clutter response to $\mathbf{s}_{tr,l}(f_q)$, and $\mathbf{x}_{n,l}(f_q)$ is an additive white Gaussian noise term distributed with:

$$\mathbf{x}_{n,l}(f_q) \sim \mathcal{CN}\left(0, \sigma_n^2 \mathbf{I}_N\right). \quad (23)$$

We assume that the clutter has the spatial distribution $\mathbf{H}_{c,l'}^T(f_q)$ as the reverse clutter channel that is independent of the forward clutter channel. Thus,

$$\begin{align}
\mathbf{x}_{c,l}(f_q) &= \mathbf{H}_{c,l'}^T(f_q)\mathbf{s}_{tr,l}(f_q), & (24)\\
&\sim \mathcal{CN}\left(0, \mathbf{R}_{x,c}(f_q)\right), & (25)
\end{align}$$

where the covariance matrix $\mathbf{R}_{x,c}(f_q)$ is defined by:

$$\mathbf{R}_{x,c}(f_q) = E\left\{\mathbf{H}_{c,l'}^T(f_q)\mathbf{s}_{tr,l}(f_q)\mathbf{s}_{tr,l}^H(f_q)\mathbf{H}_c^*(f_q)\right\}. \quad (26)$$

IV. MIMO DETECTORS IN CLUTTER

Time Reversal (TR-MIMO) Detector. From (26), we define

$$\begin{align}
\mathbf{R}_1(f_q) &= \frac{1}{\sigma_n^2}\mathbf{R}_{x,c}(f_q) + \mathbf{I}_N, & (27)\\
\tilde{\mathbf{x}}_l(f_q) &\triangleq [\tilde{X}_{l,1}(f_q), \cdots, \tilde{X}_{l,N}(f_q)]^T & (28)\\
&= \mathbf{R}_1^{-\frac{1}{2}}(f_q)\mathbf{x}_l(f_q) & (29)\\
&= \tilde{\mathbf{c}}_l(f_q) + \mathbf{w}_l(f_q) & (30)
\end{align}$$

where

$$\begin{align}
\tilde{\mathbf{c}}_l(f_q) &= \mathbf{R}_{x,c}^{-\frac{1}{2}}(f_q)\overline{\mathbf{H}}^T(f_q)\mathbf{s}_{tr,l}(f_q) & (31)\\
\mathbf{w}_l(f_q) &= \mathbf{R}_1^{-\frac{1}{2}}(f_q)(\mathbf{x}_{c,l}(f_q) + \mathbf{x}_{n,l}(f_q)). & (32)
\end{align}$$

Next, using (30), employing orthogonal waveforms to matched-filter the received signals, and collecting all the frequency components, we obtain:

$$R_{l,in} \triangleq \sum_{q=0}^{Q-1} \tilde{X}_{l,i}(f_q)S_n^*(f_q) = k_l\tilde{C}_{l,in} + \tilde{W}_{l,in}, \quad (33)$$

Stacking the data (33) into vector form yields

$$\begin{align}
\mathbf{r}_l &= [R_{l,11}, R_{l,12}, \cdots, R_{l,NN}]^T & (34)\\
\tilde{\mathbf{c}}_l &= k_l[\tilde{C}_{l,11}, \tilde{C}_{l,12}, \cdots, \tilde{C}_{l,NN}]^T & (35)\\
\tilde{\mathbf{w}}_l &= [\tilde{W}_{l,11}, \tilde{W}_{l,12}, \cdots, \tilde{W}_{l,NN}]^T & (36)
\end{align}$$

The MIMO detection problem using time reversal given the l-th data vectors defined above is now formulated by

$$\begin{align}
\mathbb{H}_1 : \mathbf{r}_l &= \tilde{\mathbf{c}}_l + \tilde{\mathbf{w}}_l \\
\mathbb{H}_0 : \mathbf{r}_l &= \tilde{\mathbf{w}}_l
\end{align} \quad , l = 1, \ldots, L. \quad (37)$$

Under $\mathbb{H}_0$, the clutter return is

$$\begin{align}
\mathbf{x}_{c,l}'(f_q) &= \mathbf{H}_{c,l'}^T(f_q)k_l'\left[\mathbf{P}_{\mathbf{A}(f_q)}\mathbf{v}_l(f_q)\right]^* & (38)\\
k_l'^2 &= QNE_s/\sum_{q=0}^{Q-1}\left\|\mathbf{P}_{\mathbf{A}(f_q)}\mathbf{v}_l(f_q)\right\|^2. & (39)
\end{align}$$

Hence $\mathbf{R}_1(f_q)$ should take a slightly different from from (28). We consider the energy detector:

$$\ell_{\text{TR-MIMO}}(\mathbf{r}_l) = \|\mathbf{r}_l\|^2 = \sum_{i=1}^{N}\sum_{n=1}^{N}|R_{l,in}|^2 \quad (40)$$

Conventional or Statistical (S-MIMO) detector. For conventional detection, the received signal at A transmitted from B is given by:

$$\begin{align}
\mathbf{y}_l(f_q) &\triangleq [Y_{l,1}(f_q), \cdots, Y_{l,N}(f_q)]^T & (41)\\
&= \overline{\mathbf{H}}^T(f_q)\mathbf{s}_B(f_q) + \mathbf{y}_{c,l}(f_q) + \mathbf{y}_{n,l}(f_q) & (42)
\end{align}$$

where $\mathbf{y}_{c,l}(f_q) = \mathbf{H}_{c,l'}^T(f_q)\mathbf{s}_B(f_q)$. To mitigate the clutter, we let

$$\begin{align}
\mathbf{R}_{c,y}(f_q) &= E\left\{\overline{\mathbf{H}}^T(f_q)\mathbf{s}_B(f_q)\mathbf{s}_B^H(f_q)\overline{\mathbf{H}}^*(f_q)\right\} & (43)\\
\mathbf{R}_2(f_q) &= \frac{1}{\sigma_n^2}\mathbf{R}_{c,y}(f_q) + \mathbf{I}_N. & (44)
\end{align}$$

Next, we let

$$\begin{align}
\mathbf{z}_l(f_q) &\triangleq [Z_{l,1}(f_q), \cdots, Z_{l,N}(f_q)]^T & (45)\\
&= \mathbf{R}_2^{-\frac{1}{2}}(f_q)\mathbf{y}_l(f_q) = \mathbf{h}_l(f_q) + \mathbf{v}_l(f_q). & (46)
\end{align}$$

We construct the detector similar to the detector in [1]. Using (46) and matched filtering the received signals with orthogonal waveforms yields

$$U_{l,in} = \sum_{q=0}^{Q-1} Z_{l,i}(f_q)S_n^*(f_q) = \tilde{H}_{l,in} + \tilde{V}_{l,in}, \quad (47)$$

Again, the transmitting waveforms are quasi-orthogonal. Grouping $U_{l,in}$ into $N^2 \times 1$ vectors yields

$$\begin{align}
\mathbf{u}_l &= [U_{l,11}, U_{l,12}, \cdots, U_{l,NN}]^T, & (48)\\
\tilde{\mathbf{h}}_l &= [\tilde{H}_{l,11}, \tilde{H}_{l,12}, \cdots, \tilde{H}_{l,NN}]^T, & (49)\\
\tilde{\mathbf{v}}_l &= [\tilde{V}_{l,11}, \tilde{V}_{l,12}, \cdots, \tilde{V}_{l,NN}]^T. & (50)
\end{align}$$

Thus, the binary hypothesis test for S-MIMO is given by

$$\begin{align}
\mathbb{H}_1 : \mathbf{u}_l &= \tilde{\mathbf{h}}_l + \tilde{\mathbf{v}}_l \\
\mathbb{H}_0 : \mathbf{u}_l &= \tilde{\mathbf{v}}_l
\end{align} \quad , l = 1, \ldots, L. \quad (51)$$

We consider the energy detector:

$$\ell_{\text{S-MIMO}}(\mathbf{u}_l) = \|\mathbf{u}_l\|^2 = \sum_{i=1}^{N}\sum_{n=1}^{N}|U_{l,in}|^2 \quad (52)$$
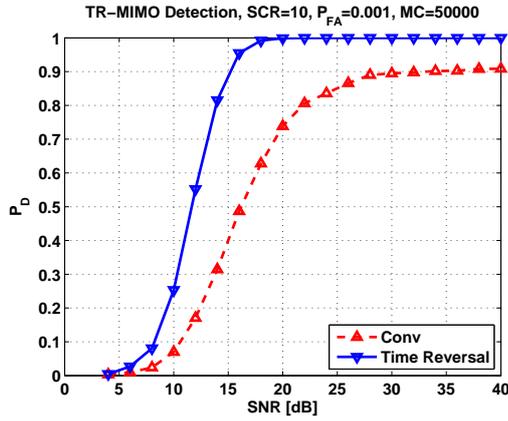
TR–MIMO Detection, SCR=10, P_FA=0.001, MC=50000

Fig. 1. Probability of Detection vs. SNR for both the Conventional and Time Reversal (TR) based detectors, for the case where SCR=10dB. MC=50,000 Monte Carlo trials were conducted. TR shows an SNR gain of 7dB at $P_D 0.8$.

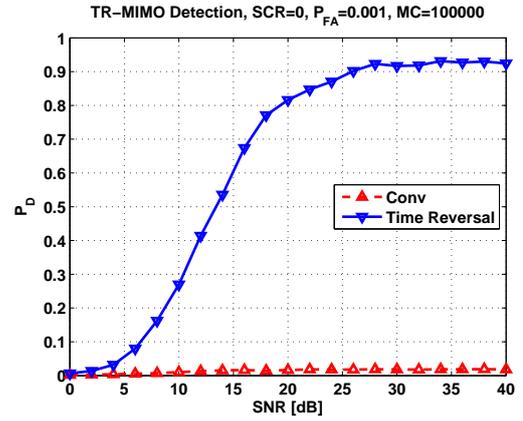**TR–MIMO Detection, SCR=0, P_FA=0.001, MC=100000**

Fig. 2. Probability of Detection vs. SNR for both the Conventional and Time Reversal (TR) based detectors, for the case where SCR=0dB. MC=100,000 Monte Carlo trials were conducted. TR saturates performance at $P_D = 0.93$, while the Conventional detector saturates at $P_D = 0.02$.

V. SIMULATIONS

In this section, we carry out numerical simulations to evaluate the performance of the proposed TR-MIMO detector. We use two transmit antennas and two receive antennas ($N = 2$), four independent frequency samples ($Q = 4$), a rank 1 target subspace ($p = 1$), and fully channel coherence ($\rho = 1$). The clutter spatial covariance term is $\lambda = .1$. The false alarm rate is $P_{fa} = 0.001$. The signal to noise ratio (SNR) and the signal to clutter ratio (SCR) are defined as follows, respectively,

$$\text{SNR} = \frac{\sum_{q=0}^{Q-1} 2NE_s\sigma_s^2(f_q)p}{N\sigma_n^2} \quad (53)$$

$$\text{SCR} = \frac{\sum_{q=0}^{Q-1} \sigma_s^2(f_q)p}{\sum_{q=0}^{Q-1} \sigma_c^2(f_q)\text{tr}\mathbf{\Lambda}}. \quad (54)$$

In figure 1, we plot the Probability of Detection (P_D) for both Time Reversal and Conventional detectors in the case where $\text{SCR} = 10$ dB. Time Reversal shows improved performance, with an effective SNR gain of 7dB at $P_D = 0.8$. Furthermore, the Conventional detector saturates at $P_D = 0.91$, signaling a failure to compensate for clutter contributions. We repeated the experiment with $\text{SCR} = 0$ dB; the results are shown in figure 2. While Time Reversal suffers an SNR loss of 6dB (at $P_D = 0.8$) as compared with the first test and saturates at $P_D = 0.93$, the Conventional detector saturates at $P_D = 0.02$. This shows that Time Reversal provides better detection performance and is more robust to increasing clutter.

VI. CONCLUSION

In this paper, we derive a subspace-based method for detection of a target using Time Reversal for Multi-Input Multi-Output radar in the presence of full rank multipath clutter. We have conducted numerical simulations to verify this approach. These studies show that TR-MIMO outperforms the conventional detector derived for the same scenario.

REFERENCES

[1] Y. Jin, J. M. F. Moura, and N. O'Donoughue, "Time Reversal transmission in Multi-Input Multi-Output Radar," *IEEE Journal of Selected Topics in Signal Processing*, vol. 4, no. 1, pp. 210–225, February 2010.

[2] M. J. D. Rendas and J. M. F. Moura, "Cramér-Rao bounds for location systems in multipath environments," vol. 39, no. 12, pp. 2593–2610, December 1991.

[3] M. R. Bell, "Information theory and radar waveform design," vol. 39, no. 5, Sept. 1993.

[4] S. Sen and A. Nehorai, "OFDM MIMO radar with mutual-information waveform design for low-grazing angle tracking," *IEEE Transactions on Signal Processing*, vol. 58, no. 6, pp. 3152 – 3162, June 2010.

[5] E. Fishler, A. Haimovich, R. Blum, D. Chizhik, L. Cimini, and R. Valenzuela, "MIMO radar: An idea whose time has come," in *Proc. IEEE Radar Conf.*, April 2004, pp. 71–78.

[6] G. J. Frazer, Y. I. Abramovich, and B. A. Johnson, "Spatially waveform diverse radar: perspectives for high frequency OTHR," in *IEEE Radar Conf.*, April 2007.

[7] Y. Jin and J. M. F. Moura, "Time-Reversal detection using antenna arrays," *IEEE Trans. on Signal Processing*, vol. 57, no. 4, pp. 1396–1414, April 2009.

[8] J. M. F. Moura and Y. Jin, "Detection by Time Reversal: Single antenna," *IEEE Trans. on Signal Processing*, vol. 55, no. 1, pp. 187–201, January 2007.

[9] Y. Jin and J. M. F. Moura, "Time Reversal imaging by adaptive interference canceling," *IEEE Trans. on Signal Processing*, vol. 56, no. 1, pp. 233–247, January 2008.

[10] M. Skolnik, *Introduction to Radar Systems*, 3rd ed. New York, NY: IMcGraw Hill, 2002.

[11] Van Trees, *Detection, Estimation, and Modulation Theory, Part III: Radar-Sonar Signal Processing and Gaussian Signals in Noise*. Wiley-Interscience, 2001.

[12] E. J. Barlow, "Doppler Radar," *Proceedings of the IRE*, vol. 37, no. 4, pp. 340–355, April 1949.

[13] J. L. Wong, I. S. Reed, and Z. A. Kaprielian, "A model for the radar echo from a random collection of rotating dipole scatterers," *IEEE Trans. on Aerospace and Electronic Systems*, vol. 3, no. 2, pp. 171–178, March 1967.

[14] C. Prada, S. Manneville, D. Spoliansky, and M. Fink, "Decomposition of the time reversal operator: Detection and selective focusing on two scatterers," *J. Acoust. Soc. Am.,*, vol. 99, no. 4, pp. 2067–2076, April 1996.

[15] M. E. Yavuz and F. L. Teixeira, "Full time-domain DORT for ultra-wideband electromagnetic fields in dispersive, random inhomogeneous media," *IEEE Trans. on Antennas and Propagation*, vol. 54, no. 8, pp. 2305–2315, 2006.